The near-field method for dynamic analysis of structures on soft soils including inelastic soil–structure interaction

M. Ghandil, F. Behnamfar *

Department of Civil Engineering, Isfahan University of Technology, Esfahan 8415683111, Iran

A B S T R A C T

The problem of soil–structure interaction analysis with the direct method is studied. The direct method consists of explicitly modeling the surrounding soil to bedrock and the structure resting on the soil. For the soil medium, usually the traditional equivalent linear method with a reduced shear modulus and an increased damping ratio for the soil is used. However, this method does not work in the vicinity of foundation where the soil behavior is highly nonlinear because of presence of large strains. This research proposes a modified equivalent linear method with a further reduction of the soil shear modulus in the near-field of foundation that results in validity of using the equivalent linear method throughout. For regular short, intermediate and tall structures resting on such soft soils, a series of dynamic time-history analysis is implemented using earthquake records scaled to a sample design spectrum and the nonlinear structural responses are compared for different assumptions of soil behavior including the elasto-plastic Mohr–Coulomb, the traditional equivalent linear, and the proposed modified equivalent linear method. This analysis validates the proposed method.

© 2015 Elsevier Ltd. All rights reserved.

1. Introduction

In the direct method of analysis of soil–structure interaction (SSI) it is needed to model both the underlying soil and the structure accurately since they are to be analyzed together. The structure is a bounded medium and can be currently modeled to almost any practical level of accuracy. On the other hand, two important obstacles emerge when modeling the soil: its unlimited dimensions and its nonlinear behavior from very small strains. To resolve the problem of unboundedness of soil medium, the soil is usually made limited to a rigid bedrock at the bottom and two vertical artificial boundaries on the two sides. As of the material behavior of soil, in SSI analysis usually the soil is assumed to behave linearly but the stiffness and damping properties of soil are modified to be consistent with the average strain level in each layer. This method is known as the equivalent linear method (ELM). While the ELM has the great advantage of highly simplifying the SSI analysis, it may not be suitable to be used for the soil in the vicinity of foundation, where the strain level is too high for the ELM to be accurate enough. However, this fact is often ignored and the ELM is used for the total soil medium.

Taking the above issues into account, one should not forget that the final purpose of an SSI analysis is usually computing the design responses of structure, not the soil. The time and effort spent on soil modeling whether as an artificially bounded medium or as springs and dampers attached to the foundation might not be worth it always. Therefore, having other valid means to assess the effect of soil flexibility on detailed story responses of a structure and to decide whether more rigorous approaches should be taken or not, can prove to be valuable.

Regarding modeling the soil in vicinity of foundation, researchers have mainly adopted two approaches. In the first approach, it is proposed to divide the soil into a nonlinear near field zone with an arbitrary geometry, and a linear far-field zone. The second approach is to use a very thin contact zone or contact elements around foundation with nonlinear behavior. Wolf [1] presented a near-field nonlinear zone to be modeled with the finite element method (FEM) bounded with an arbitrary boundary and calculated the exact dynamic stiffness of the boundary in the frequency domain or the reactions in time domain. The method was called the cell method and later the scaled boundary FEM. Casciati and Borja [2] analyzed the SSI of the Aga Memnon sculpture located in Egypt. First they used the Shake91 program and implemented a free-field analysis for the site. Then the effective shear modulus and damping ratio of soil, extracted from Shake91, was used in developing the three dimensional (3D) model of the soil and the sculpture. To compensate for

* Corresponding author.
  E-mail address: farhad@cc.iut.ac.ir (F. Behnamfar).

Table 1
The typical sections of 5 to 30-story buildings (units in mm, IPE*a* is an I section, *a* mm deep).

No. of stories	Beam sections	Column sections
5	IPE 300 and 330	Box 240 × 12.5, 260 × 12.5 and 280 × 12.5
10	IPE 300, 330 and 360	Box 260 × 20, 280 × 20 and 300 × 20
15	IPE 300, 300O, 330, 330O, 360 and 360O	Box 180 × 20, 240 × 20, 300 × 20 and 340 × 20
20	IPE 300, 300O, 330, 330O, 360 and 360O 2IPE 300 and 2IPE 330	Box 200 × 20, 240 × 20, 260 × 20, 320 × 20 and 340 × 20
25	IPE 300, 300O, 330, 330O, 360 and 360O 2IPE 300 and 2IPE 330	Box 240 × 20, 280 × 20, 340 × 20 and 360 × 20
30	IPE 300, 300O, 330, 330O, 360 and 360O 2IPE 330, 2IPE 360 and 2IPE360O	Box 280 × 40, 320 × 40, 340 × 20, 360 × 40 and 380 × 40

Table 2
Characteristics of the pile groups designed.

Soil type	No. of piles for each building		Pile diameter for each building (m)				Pile cap thickness (m)
	15S and 20S	25S and 30S	15S	20S	25S	30S	
C	16	25	0.4	0.5	0.6	0.7	0.8
D	16	25	0.5	0.6	0.7	0.8	1.0
E	25	25	0.5	0.6	0.8	0.9	1.2

the effect of the structure on the characteristics of the soil underneath, contact elements were introduced at the base of the structure. Emani and Maheshvari [3] utilized the cell method and by dividing the soil into a zone around piles and the outer zone, calculated the impedance functions of group piles in homogeneous elastic soils. Manna and Baidya [4] used near-field cylindrical elements around piles to compare the dynamic response with that derived by in situ vibration tests. In their work, assigning the equivalent linear properties was limited to the near-field soil and the rest of the soil was assumed to be linear. They reported a good accuracy for their analytical model.

The research on structural response on flexible soil is a vast area. To name just a recent few, the following works are mentioned. Dutta et al. [5] studied an SDF superstructure resting on concentrated springs. They concluded that the effects of SSI appear as increase of base shear for short buildings and its reduction for intermediate and tall structures. These effects fade out as the soil stiffness increases. Wegner et al. studied the SSI of a single 30-story building [6]. Use was made of the FEM for modeling the near-field soil and the scaling (cell) method of Wolf [1] for the boundary of the far-field medium. They reported that the story drifts increase due to the increased inertial forces initiated by the rocking motion of foundation. Nakhaei and Ghannad examined an SDF model resting on concentrated springs [7]. The soil behavior was assumed to be linear and elastic. They observed an increased damage index because of SSI. Chau et al. [8] studied the nonlinear interaction between pile foundations and their surrounding soil experimentally. They concluded that a seismic pounding event between the laterally compressed soil and the pile near the pile cap was responsible for pile damage around the same locations. Gajan et al. [9] applied a beam-on-nonlinear-Winkler foundation model and a contact interface model as practical tools for nonlinear soil foundation interaction analysis. They reported generally consistent moment–rotation behavior with their models. Pitilakis and Clouteau [10] proposed an equivalent linear substructure

Roof (Elv. +45)

Freefield (Elv. 0)

Pile Bot. (Elv. -20)
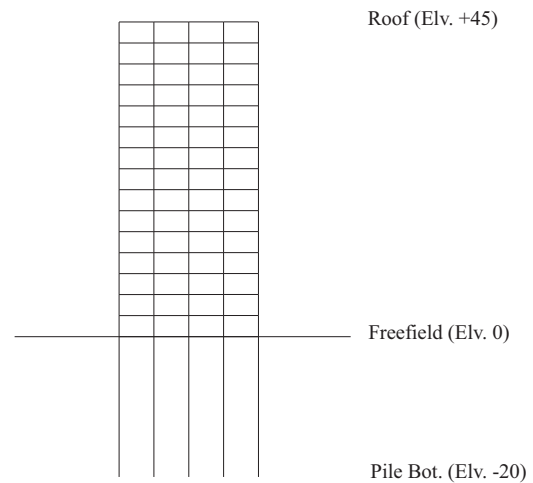
Fig. 1. Elevation view of the 15-story building.

approximation for the SSI problem including a nonlinear soil and an elastic structure. They validated their theoretical model through centrifuge tests. Raychowdhury [11] studied the nonlinear behavior of the soil-foundation interface in an SSI problem using a beam-on-nonlinear-Winkler-foundation (BNWF) approach and observed reduced response demands due to foundation nonlinearity. Romero et al. [12] introduced a non-linear contact condition for an SSI problem within a 3D non-linear time domain combining FEM and the boundary element method (BEM) approaches.

In the present study, a simple method is proposed for identifying an equivalent linear zone around the foundation taking into account the highly nonlinear behavior of soil in the same location due to inertial effect of structure. Utilizing the proposed method and a series of 3D analysis of several multistory buildings on soft soils with the direct method and accounting for soil plasticity, the validity of the proposed modified equivalent linear soil modeling method in accurate prediction of structural responses is evaluated for earthquake records scaled to a sample design spectrum.

2. Properties of the buildings considered

In order to study a broad height range of steel structures, six 3D buildings with 5, 10, 15, 20, 25, and 30 stories are considered. The interstory height is equally 3 m resulting in the total height of the buildings to be 15–90 m. The structures are located in a very high seismicity area. The gravitational loads are DL=7.60 kN/m^2 and

LL=2.00 kN/m^2, with DL for dead load and LL for live load. The load bearing system is a 3D special steel moment frame designed based on AISC-05. The diaphragms are RC slabs 0.15–0.25 m thick, with the thicker slabs for the taller buildings, and are assumed to be rigid in plane. The structural sections used for the buildings are summarized in Table 1.

Strip and mat foundations are used for 5 and 10-story buildings, respectively; but for the tall 15 to 30-story buildings pile group foundations are selected. The above foundation systems are all assumed to have a boundary area of 21 m × 21 m. Length of each pile is 20 m. Stiff to soft soils are considered separately in this study as the soil types C, D, and E [13]. Table 2 shows the characteristics of the pile groups designed for each building and each soil type.

Fig. 1, as an example, shows the elevation of the 15-story building and its group of piles in soil type D.

3. Geotechnical considerations

Six different cases of ground including three soil types C, D, and E [13] corresponding to stiff to soft soils, respectively, and two soil profiles I and II for each soil type, are considered. Profile I consists of two sand layers with a total thickness of 25 m on bedrock. Profile II includes three different clay layers with a total thickness of 45 m resting on bedrock. The mechanical characteristics of the different soil types/layers are mentioned in Table 3. The weighted-average shear wave velocity, using thickness of the layers down to a depth of 30 m as the weight function, is also mentioned for each case. The average fundamental period of the soil layers, T_s, is calculated using the mentioned average shear wave velocity and the common relation $T_s=4H/V_{s,ave}$, where H is the total thickness of the soil layers.

The hardening of soil under the static action of building weight in the vicinity of foundation and softening of soil for larger seismic shear strains throughout the layers are considered when doing dynamic analysis in this study. This is done with proper adjustments for the shear modulus G. To adjust for the static effects, the shear modulus at a certain depth is augmented proportional to the ratio of the effective stress at that depth including the building weight to the same value without the building weight effect [14]. For the dynamic large strain effect, the shear modulus at each depth is decreased as a function of a fraction of the maximum shear strain at the same depth using the curves provided in Ref. [15] for clays and sands.

Fig. 2 shows the amplification curves of the sites consisting of the soil type D as an example. As observed, the selected sites well amplify the bedrock motions for the common frequency range of earthquakes at bedrock of 0.1–10 Hz.

The dynamic characteristics of the sites presented in Table 3 and Fig. 2 (and alike) show that the selected soil profiles are general enough within the soil types considered.

4. Selection and modification of earthquake records

Three sets of consistent seismic records, each containing 10 accelerograms, are selected from the PEER Strong Motion Database [16] according to ASCE7-10 [13]. The criteria for selection ensuring consistency of the records are as mentioned in Table 4.

The scaling of the ground motions has been done based on ASCE7-10 for each independent earthquake, such that each scaled response spectrum abscissa is not less than the design response spectral corresponding value for periods ranging from 0.2 T to 1.5 T where T is the fundamental period of the (fixed-base) building. Apart from the fact that this is a prescribed code-based approach, it is done to account

Table 3
Properties of the soil layers (Z=depth, E=modulus of elasticity, G_{max}=static shear modulus, V_s=shear wave velocity, T_s=fundamental period, C_u=undrained cohesion, Ø=friction angle, $V_{s,ave}$=weighted-average shear wave velocity).

(a) Soil type C
Profile I: sand

Z (m)	Ø (°)	E (KPa)	G_{max} (KPa)	V_s (m/s)	$V_{s,ave}$ (m/s)	T_s (s)
0–10	35	988,659	366,170	439	563	0.18
10–25	39	2,260,489	837,218	647		

Profile II: clay

Z (m)	C_u (KPa)	E (KPa)	G_{max} (KPa)	V_s (m/s)	$V_{s,ave}$ (m/s)	T_s (s)
0–10	225	935,348	346,425	427	527	0.34
10–25	313	1,177,933	436,272	473		
25–45	555	1,873,373	693,842	589		

(b) Soil type D
Profile I: sand

Z (m)	Ø (°)	E (KPa)	G_{max} (KPa)	V_s (m/s)	$V_{s,ave}$ (m/s)	T_s (s)
0–10	30	175,446	64,980	190	244	0.43
10–25	35	402,192	148,960	280		

Profile II: clay

Z (m)	C_u (KPa)	E (KPa)	G_{max} (KPa)	V_s (m/s)	$V_{s,ave}$ (m/s)	T_s (s)
0–10	148	166,334	61,605	185	228	0.84
10–25	206	204,242	75,645	205		
25–45	365	333,578	123,548	255		

(c) Soil type E
Profile I: sand

Z (m)	Ø (°)	E (KPa)	G_{max} (KPa)	V_s (m/s)	$V_{s,ave}$ (m/s)	T_s (s)
0–10	24	27,926	10,343	78	100	1.00
10–25	30	64,274	23,805	115		

Profile II: clay

Z (m)	C_u (KPa)	E (KPa)	G_{max} (KPa)	V_s (m/s)	$V_{s,ave}$ (m/s)	T_s (s)
0–10	82	14,913	5523	57	70	2.57
10–25	114	18,218	6747	63		
25–45	202	29,568	10,951	78		

for the higher mode effects with applying the lower period factor of 0.2, and for nonlinearity of building's response with the upper period factor of 1.5. The records used, their original PGA, and the scale factors in each case are shown in Table 5.

For instance, Fig. 3 shows the spectral accelerations of the soil type D records before and after scaling for the 10-story building with $T = 2.03$ s. Moreover, comparison with Fig. 2 reveals that the selected earthquakes are powerful enough in the governing frequency range of the sites.

In Section 5.3 it is mentioned that the earthquake records are input at the bedrock to the soil–structure system. Therefore it will be necessary to make a free-field response analysis beforehand, with the above ground surface motions being input at the top of a 1-D free-field soil column, consisting of the whole vertical profile of soil, to compute the ground motion at the bedrock.

5. Modeling of the system for dynamic analysis

Inelastic structures resting on equivalent linear soils are considered for the purposes of this study. The modeling is implemented in SAP2000 [17]. Fig. 4 shows the 3D model of the 30-story building on soil profile II as an example.

5.1. The free-field response analysis

The 1D dynamic analysis of the free-field site is implemented for 360 cases (6 sites and 10 records scaled for 6 structures) with Shake91 software [18]. Referring to Table 5, the ground motion is input at the surface and the bedrock motion is calculated using the ELM. One of the 360 calculated bedrock motions is shown in Fig. 5 along with the original ground motion recorded at the surface.
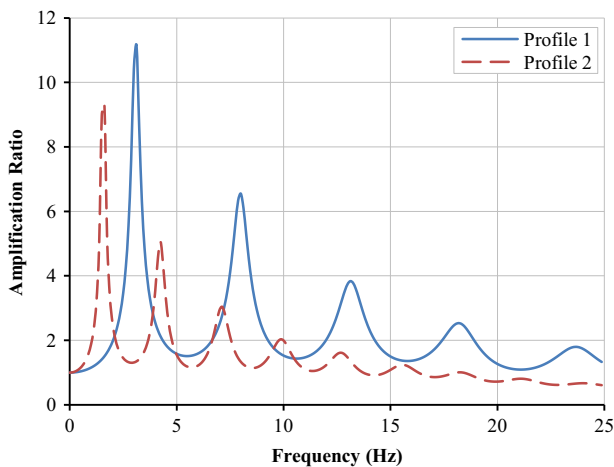
Fig. 2. Amplification curves of the sites associated with the soil type D.

5.2. Modeling of the structure

The beams and columns of the frames can exhibit inelastic behavior. Such a nonlinear behavior is introduced to the structural members by placing elasto-plastic zero length hinge elements at the ends of the frame elements. These hinges are rigid before yield. Their moment–rotation behavior is schematically shown in Fig. 6. This is a sample figure in which the quantities on the vertical and horizontal axes are normalized using appropriate scale factors (SF's).

In Fig. 6, B is the yield point and C is the capacity point where afterwards the moment capacity drops sharply due to local failures (rupture or buckling). The length of BC is proportional to the rotation ductility of the hinge. This in turn is a function of the beam or column end details and the level of the shear and axial forces in members. Local buckling and large demand-capacity ratios (DCR) of shear and/or axial forces can considerably decrease the ductility of the plastic hinges. It is assumed that local buckling is prevented by using suitable details at the ends of members. Also, shear capacity of the members is assumed to be large enough to keep the shear DCR at small values. On the other hand, the effect of axial force in columns on reducing the ductility of the hinges is considered. As the beam-column connections are regarded to be stiff, the end-beam hinges are placed in the beam at the distance of d_b from the side of column where d_b is the beam depth. The ordinates of the anchor points on the moment–rotation diagram of Fig. 6 are extracted from ASCE41 (2006).

For the floor diaphragms and pile caps, linear shell elements are utilized. The damping matrix is assumed to be of Rayleigh type with a 5% material damping for both the structure and the original soil.

5.3. Soil partitioning and the transmitting boundaries

As mentioned earlier, the ELM [19] is used for simulating the actual nonlinear soil behavior. It has to be mentioned that for large 3D problems, such as the present study with several (360) calculation cases, ELM is the only practical method. Here the ELM is implemented in SAP2000 as follows. First, the entire soil medium is divided into a number of partitions. The shear modulus G and damping ratio ξ of soil are set to be constant in each partition. The partitioning has to be carried out with care. Specifically, the size of the partitions must be smaller at locations just below the structure and over the bedrock, because of stress concentration due to soil's deformation constraints. Each geotechnical layer of the sites is divided into two sub-layers and then is divided into partitions. Each partition is divided into 8-node 3D solid cubic elements. As a minimum of six elements should be present along the minimum important wave length [20], corresponding to a maximum important frequency of 10 Hz, the appropriate dimension of the mentioned elements is calculated to be 8.8, 3.8, and 1.2 m for the soil types C, D, and E, respectively. The actual dimension is selected to be 2.5 m for the soil types C and D, and 0.625 m for the soil type E. As the first iteration, dynamic analysis begins with using G_{max} values of Table 3 for the shear modulus of layers and a uniform damping ratio of 0.05. The average shear strain in each partition is calculated as a result and utilized to determine the new values of G

Table 4
The criteria for selection of earthquake records.

Accelerogram location	Ground level	Magnitude (Ms)	6–7
Frequency bandwidth (Hz)	0.15–10	Source distance (km)	20–50
Site classifications (ASCE7-10)	C, D, E ($V_s \leq 650$ m/s)	Strong motion duration (s)	≥ 12

Table 5
The selected earthquakes and their scale factors.

Record No.	Event	Station	PGA (g)	Scale Factor					
				5 Story	10 Story	15 Story	20 Story	25 Story	30 Story
(a) Soil Type C									
C1	Gazli, USSR	Karakyr	0.6438	1.09	1.15	1.20	1.26	1.32	1.38
C2	Landers	Lucerne	0.7214	1.43	1.50	1.58	1.65	1.73	1.80
C3	Loma Prieta	LGPC	0.7835	0.80	0.84	0.89	0.93	0.97	1.01
C4	Cape Mendocino	Cape Mendocino	1.3455	1.18	1.25	1.31	1.37	1.43	1.50
C5	Chi-Chi, Taiwan	TCU067	0.4068	1.11	1.16	1.22	1.28	1.34	1.40
C6	Northridge-1	Jensen Filter Plant Generator	0.7649	0.94	0.99	1.04	1.08	1.13	1.18
C7	Chi-Chi, Taiwan	CHY006	0.3596	1.38	1.45	1.52	1.59	1.67	1.74
C8	Loma Prieta	Saratoga -W Valley Coll.	0.3111	1.43	1.50	1.58	1.65	1.73	1.80
C9	Tabas, Iran	Tabas	0.8128	0.67	0.71	0.74	0.78	0.81	0.85
C10	Northridge-1	LA Dam	0.4528	1.38	1.45	1.52	1.59	1.67	1.74
(b) Soil Type D									
D1	Imperial Valley-06	El Centro Differential Array	0.431	1.36	1.44	1.51	1.58	1.65	1.72
D2	Loma Prieta	Hollister Diff. Array	0.264	1.80	1.89	1.99	2.08	2.17	2.27
D3	Kocaeli, Turkey	Duzce	0.326	1.35	1.42	1.49	1.57	1.64	1.71
D4	Duzce, Turkey	Duzce	0.427	0.97	1.02	1.07	1.12	1.17	1.22
D5	Chi-Chi, Taiwan	CHY036	0.260	1.60	1.69	1.77	1.86	1.94	2.02
D6	Erzican, Turkey	Erzincan	0.489	1.20	1.26	1.33	1.39	1.45	1.52
D7	Imperial Valley-06	El Centro Array #7	0.463	1.22	1.28	1.34	1.41	1.47	1.54
D8	Loma Prieta	Foster City - APEEL 1	0.291	1.76	1.85	1.95	2.04	2.13	2.22
D9	Northridge-1	Northridge -17645 Saticoy St.	0.411	1.33	1.40	1.47	1.54	1.61	1.68
D10	Northridge-1	Rinaldi Receiving St.	0.634	0.89	0.94	0.98	1.03	1.08	1.13
(c) Soil Type E									
E1	Chi-Chi, Taiwan	CHY054	0.092	4.48	4.71	4.95	5.19	5.42	5.66
E2	Kocaeli, Turkey	Ambarli	0.223	2.50	2.63	2.76	2.89	3.03	3.16
E3	Imperial Valley-06	El Centro Array #3	0.255	2.90	3.05	3.20	3.35	3.51	3.66
E4	Chi-Chi, Taiwan-04	CHY054	0.044	5.32	5.60	5.88	6.16	6.44	6.72
E5	Loma Prieta	APEEL 2 - Redwood City	0.249	3.28	3.45	3.63	3.80	3.97	4.14
E6	Chi-Chi, Taiwan	ILA004	0.072	4.64	4.88	5.12	5.37	5.61	5.86
E7	Loma Prieta	Treasure IslanE	0.132	4.15	4.37	4.59	4.81	5.03	5.24
E8	Chi-Chi, Taiwan	ILA044	0.080	5.18	5.46	5.73	6.00	6.27	6.55
E9	Loma Prieta	Foster City - MenhaEen Court	0.098	4.93	5.19	5.45	5.71	5.96	6.22
E10	Chi-Chi, Taiwan	CHY076	0.081	4.28	4.50	4.73	4.95	5.18	5.40

and ξ for the next iteration. The analysis is repeated each time with the new soil properties until convergence of the soil properties in all partitions.

The above procedure is different from what is done in Shake and is specific to this research. In Shake, as is explained in Section 5.1, no structure is present and the ELM is used for the free-field analysis with no partitioning. In SAP2000, the whole soil–structure model is calculated with partitioning as of Fig. 7. The effect of presence of the structure is taken into account for computation of effective G and ξ of the soil model. Here, the shear strain is averaged in each partition to determine the appropriate values of G and ξ for each partition. Note that in Shake the effective G and ξ values are calculated for each layer instead. Several references are available on use of SAP2000 for 3D dynamic analysis [21,22].

The bottom of the model is rigidly fixed at the bedrock surface. The vertical side boundaries are selected to be of transmitting type, where use is made of viscous dampers perpendicular to the boundary with damping factors $\rho V_s A$ in which A is the area shared by one damper, V_s is the shear wave velocity and ρ is mass density of soil. The earthquake records are only input at the bedrock to the soil–structure system.

The transmitting boundaries are usually perfect only for waves impinging the boundary perpendicularly. Determining the appropriate distance between structure and the transmitting boundary such that the reflected waves damp out before reaching to structure has been the subject of many research works. In most of the previous works, 2D plane strain soil models have been investigated. For instance, Ghosh and Wilson [23] observed that if the central distance from structure to the boundary was 3–4 and

2–3 times the equivalent radius of foundation in the horizontal and vertical directions, respectively, effect of the reflected waves was negligible.

The dimensions of the common plan of the structures in this research are $20\ \text{m} \times 20\ \text{m}$. The first try for the in-plane site dimension is a value three times the structure's dimension, i.e. 60 m, as is recommended by the above reference. Beginning from this value and increasing the dimension each time 10 m, maximum roof displacements of structures are calculated for each dimension until this value shows no sensible change. Since the largest building of this study, the 30-story building, can produce reflected waves that are likely to be the strongest ones, this building is selected for dimension analysis. For instance, the lateral displacement of the roof of this building relative to its base is presented in the following under the earthquake D7. Since the ground motion takes place in x–z plane, the plan width (y-dimension) is taken smaller to save effort. Table 6 shows the results. Because of scaling, the results for other earthquakes are also in a similar range.

As seen in Table 6, the response is stable after $L/a=3$. As a result, the sites are taken to be $80(x\text{-dir}) \times 40(y\text{-dir})\ \text{m}^2$.

6. Effects of SSI on the seismic response of soil

The seismic analysis of the system described in Sections 5.2 and 5.3 is implemented using the ELM. In Fig. 8 variation of maximum seismic soil shear strain along a column of soil located at different distances from the structure is shown for the soil type D. As
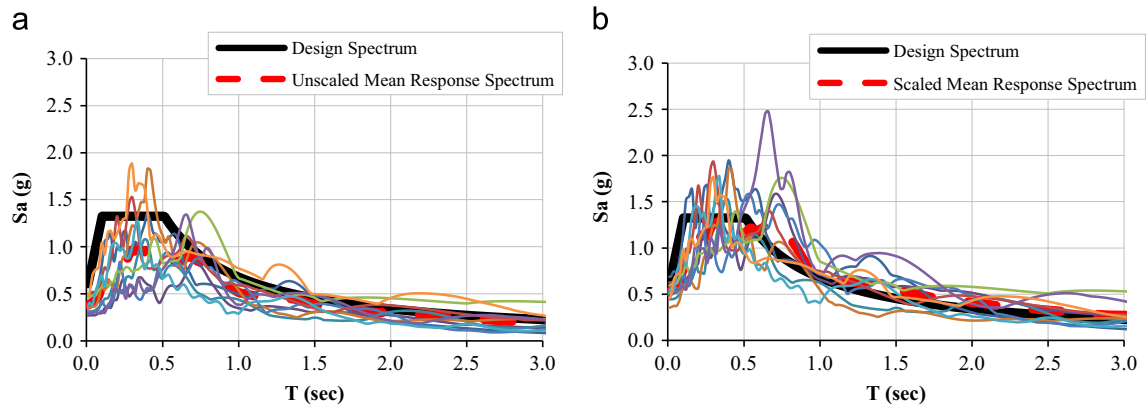
Fig. 3. Scaling of the spectral accelerations of the soil type D records for the 10-story building. (a) Before scaling. (b) After scaling.
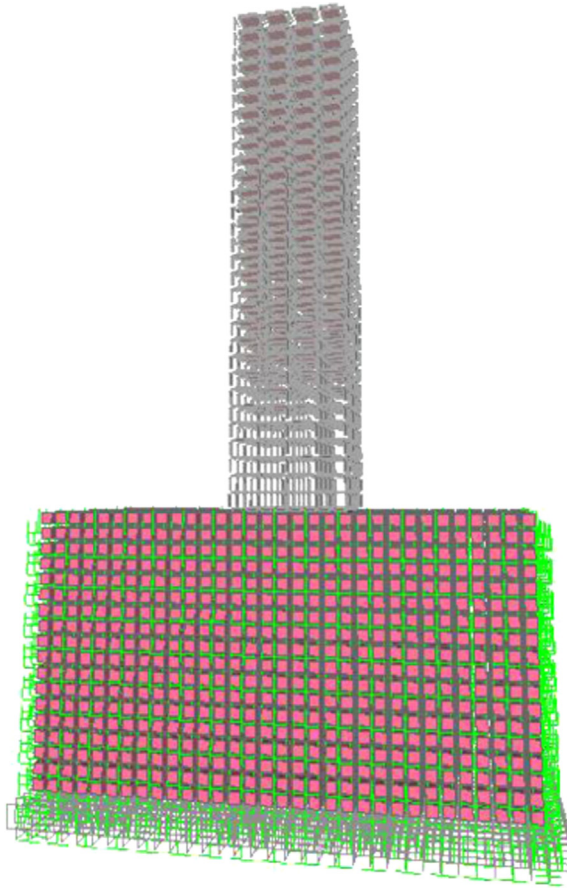
Fig.4. Modeling of structure and soil: The 30-story building on soil type II.
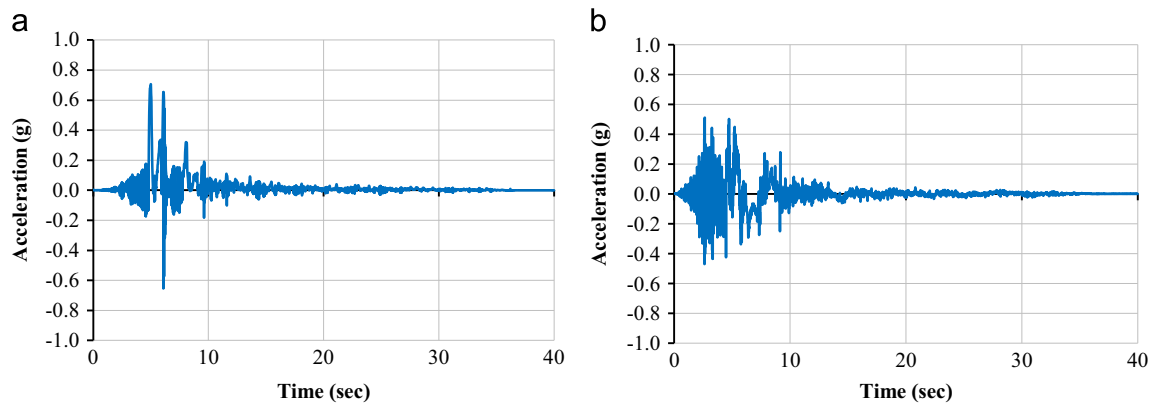
Fig. 5. The Record no. D7 (Imperial Valley earthquake; see Table 5), (a) at the ground surface; (b) at the bedrock.

observed in partitions 1 and 2, nearest to the pile cap, the seismic shear strain admits the highest level. In addition, in the same partitions, the response variation is sharp only down to a depth less than 10 m. Therefore, the soil model taken is deep enough to eliminate the boundary effects of the bedrock on the structural responses. For other structures and soil types, also, a similar situation exists (not shown). According to Ishihara [24], use of the ELM can result in accurate enough values if only the cyclic shear strain is not larger than about 0.9%. For larger strains, the soil should be modeled nonlinearly. This is the case for partitions 1 and 2 in Fig. 8.

7. Effect of material modeling of soil

Because of the results of the previous section, first the partitions 1 and 2 (Fig. 8) are modeled with a plastic constitutive relation and the other partitions with the ELM, as a nonlinear modeling of the site. Another model is also developed using the ELM throughout. Various relations have been proposed for nonlinear modeling of soil. These relations have been verified using laboratory tests on soil samples. But here the criterion is accuracy
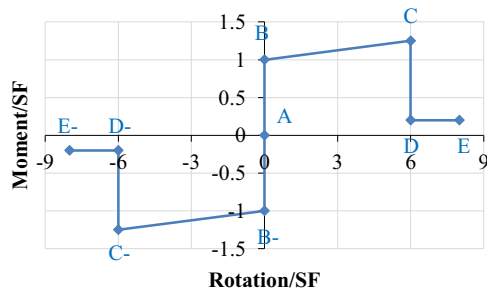
in the structural responses not the soil. It considerably reduces the sensitivity of selection of a specific soil nonlinear behavior for the purposes of this study where the criteria are accurately in prediction of structural responses with acceptable errors being up to 10% for engineering design applications. This makes the simplicity of the nonlinear soil model a prime advantage. The Mohr–Coulomb constitutive relation with post-yield hardening behavior is known as a simple nonlinear model for a rapid response analysis of soils with acceptable accuracy [25]. This model is taken in this study for analysis with ABAQUS [26].

The case of 30-story buildings on both soil profiles of the soil type D under D7 record is discussed here as an example. The lateral displacement of each story is calculated both with the nonlinear and the ELM models of soil. The ratio of the displacements calculated by the two methods is shown in Fig. 9. This figure shows that nonlinear modeling of soil in the vicinity of foundation results in an increased displacement response for the structure. The level of increase in this case is 13% at maximum and about 10% on average. The response increase shows the relative importance of plastic modeling of soil.

With the above fact in mind, the idea is to adequately decrease the equivalent linear shear modulus of soil, already calculated in the ELM, in order to achieve responses similar to the nonlinear case without need for plastic modeling, i.e., only with the ELM calculation.

This idea is tested for the above example by a further reduction of the already reduced G of the near-field soil (partitions 1 and 2, Fig. 8) in the ELM for site I by 8%. With this new shear modulus, the response is again calculated and shown in Fig. 9a. Now the difference of response between the ELM and the direct integration plastic analysis reduces considerably. Fig. 9b shows the results for the other site. Similar analyses are implemented for other cases (totally 360 cases) and the modified shear moduli are derived for all of the cases. This process is the basis of the near-field method to be presented in the next section.

Fig. 6. Schematic of moment–rotation diagram of elasto-plastic frame hinges.
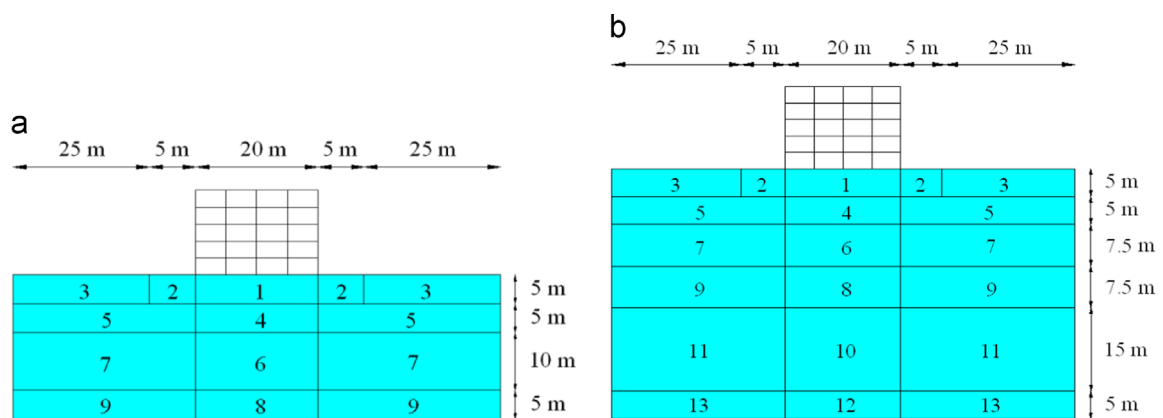
Fig. 7. Soil partitioning in 3D FEM models of SSI analysis. (a) Soil profile I; (b) soil profile II.

Table 6
The relative lateral displacement of the roof of the 30-story building on the soil type D under D7, for different site plan dimensions.

Try	Site 2 dimension		Dimension of structure in plan	L/a	B/a	Roof displacements in each try divided by that of try 4
	L (m)	*B* (m)	*a* (m)			
1	60	40	20	3	2	1.05
2	70	40	20	3.5	2	1.03
3	**80**	**40**	**20**	**4**	**2**	**1.01**
4	90	60	20	4.5	3	1.00

8. The near-field method (NFM)

8.1. Introduction

The study of the last section proves the possibility of using the simple ELM throughout the soil if a further decrease is applied on the shear modulus of the soil adjacent to surface foundation or pile cap. Since 360 cases have been studied in this research, a large bulk of data is available and can be utilized for implementation of the NFM. Fig. 10 shows the basis of the NFM. The method is based on two parameters: dimensions of the near-field, and, its shear modulus. The shear modulus of the near field will be modified based on its equivalent linear shear modulus.

8.2. Dimension of the near-field

Distribution of seismic shear strain below the foundation is the basis for determining dimensions of the near-field zone. For instance, distribution of maximum soil shear strain under D7 seismic excitation for the 30-story buildings on site II is shown in Fig. 11 for the soil type D. In part a of the figure, a rectangle

enveloping the zone with shear strains larger than 0.9% (the threshold of nonlinear analysis) is also shown. The dimensions of this rectangle can be viewed as the dimensions of the near-field zone. Part b of the figure shows the strain distribution in a 3D view with zooming on the near-field. While the volume of this zone is less than 4% of the total volume of the modeled soil medium, it has a great effect on the seismic response of structure.

Analysis similar to Fig. 11 was implemented for all 360 cases. Altogether, the cases agree that the near-field zone proceeds up to 25% of the building width on each side and at the bottom of the building.

8.3. The shear modulus of the near field

In the analysis of this section, all 360 cases were examined first with modeling the near field with the Mohr–coulomb criterion and then with the ELM. The equivalent linear properties of soil are calculated as described in Section 5.1, for the free field. Then, consecutive reductions are applied on the shear modulus of the soil in the near-field zone for the structural response to be converged to that computed with nonlinear soil modeling. The
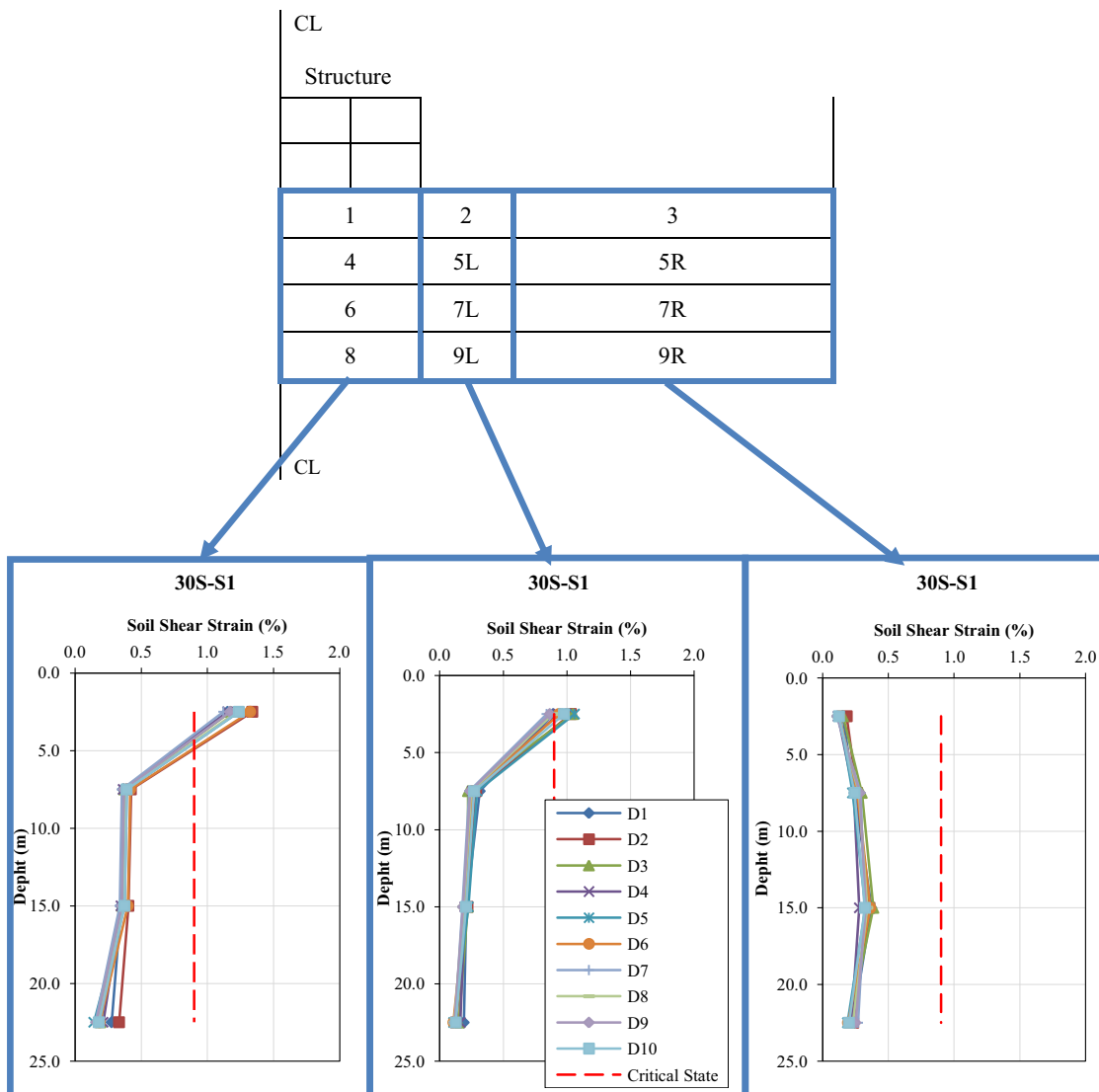
Fig. 8. Maximum seismic shear strain in different soil columns, the 30-story building, soil type D, profile I, various earthquakes.

modification factor is $\alpha_G = G_{near\text{-}field}/G_{free\text{-}field}$, where $G_{near\text{-}field}$ is the final shear modulus of the near field and $G_{free\text{-}field}$ is the effective shear modulus for the top layer of soil obtained from ELM analysis of the free field with Shake. The modification (reduction) factors are shown in Table 7 for instance for the 30-story building
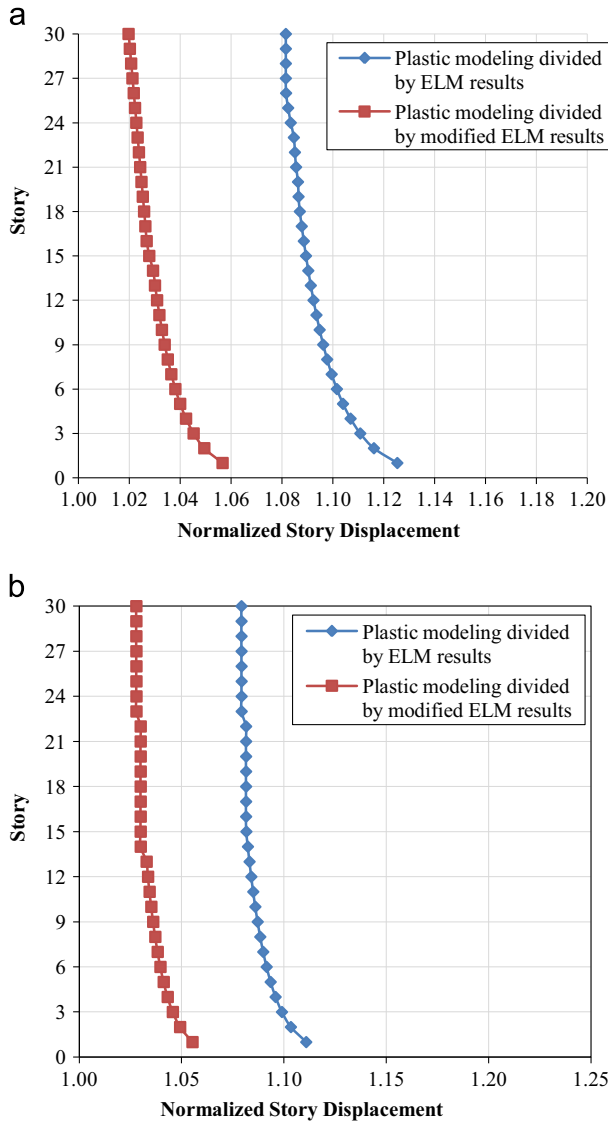
Fig. 9. Normalized response of the 30 story buildings on the soil type D with different modeling methods for the soil under earthquake D7. (a) Site I; (b) Site II.

on the soil type D under different earthquakes. The dispersion of the values is small. This is expected, as all of the records are scaled to the same spectrum, as explained in Section 4, and have an amplitude level similar to the ASCE7-10 design spectrum.

The values averaged over each set of records associated with each soil type, are shown in Fig. 12 versus the fundamental periods of the fixed-base buildings, and in Table 8 versus the number of stories. A nearly uniform reduction in the factor is observed for both sites as the height of the building increases, i.e., the taller the building, the smaller the reduced shear modulus for the same soil. This can be attributed to the larger amplitudes of the normal and therefore shear strains due to larger overturning moments of the taller buildings. On the other hand, the shear modulus ratios of Fig. 12 are smaller for tall buildings on pile groups and larger for short buildings on surface foundations. Therefore, effects of natural period and foundation type are also included.

Fig. 12 is utilized in the following to derive a regression equation for the shear modulus ratio.

8.4. A semi-analytical equation for $G_{near-field}$

Using curves of the shear modulus ratio shown in Fig. 12, a curve fitting technique is applied to derive an equation for estimating the shear modulus of the near-field zone of Figs. 10 and 11. Practically, the characteristics of the whole soil medium, especially the near-field zone, are needed in the modeling phase of the soil–structure system, i.e., before the SSI analysis is carried out. Then, the fixed-base fundamental period of structure is selected to be the basis of the regression analysis. According to Fig. 12, a 3rd order polynomial fit seems to be adequate. The general form of the fitting curve is as

$$\alpha_G = G_{near-field}/G_{free-field} = AT^3 + BT^2 + CT + 1 \tag{1}$$

In Eq. (1), T is the first mode period of the fixed-base building, and A, B and C are regression constants specific to the soil type. They are calculated as follows:

$$A = A_1(T_s) + A_2$$

$$B = B_1(T_s) + B_2$$

$$C = C_1(T_s) + C_2 \tag{2}$$

in which T_s is the first mode period of the site and the coefficients $A_1, \ldots, C_2$ are determined for each soil type using Table 9.

The relative difference between the values of α_G calculated using Eq. (1) and Fig. 12 is less than 1% for the cases considered in this study.
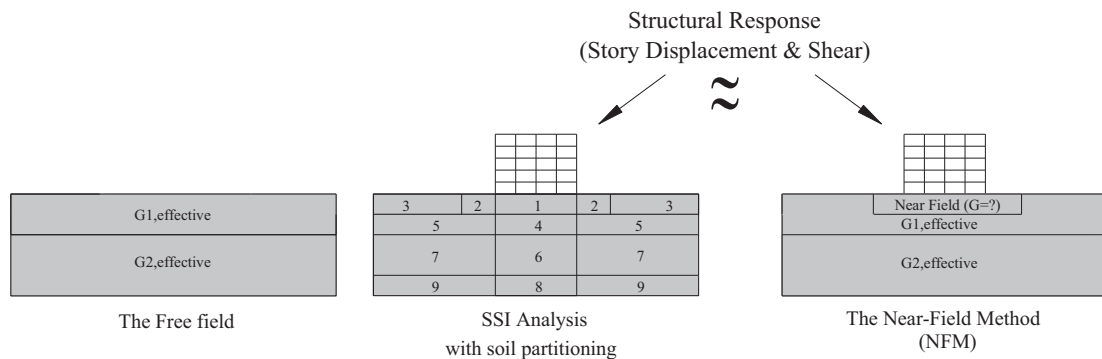
Fig. 10. Basis for the NFM.
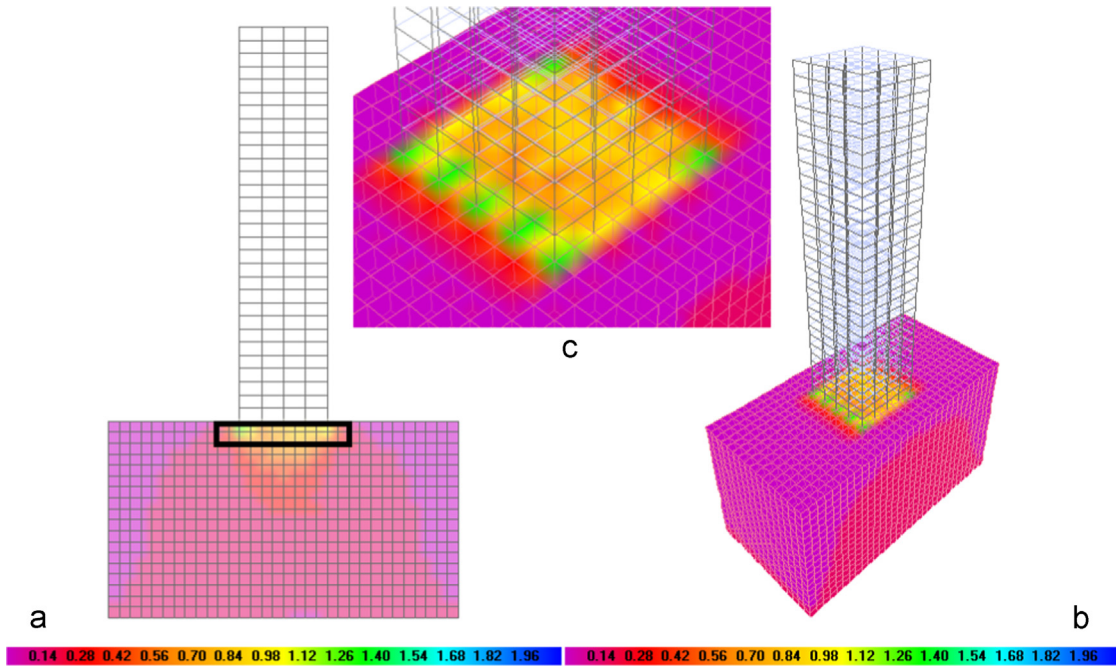
Fig. 11. The soil's seismic shear strain and the near-field zone for the 30-story building, site II, soil type D, D7 seismic excitation. (a) Cross section; (b) 3D view; (c) magnified near-field (strain values are in percent).

Table 7
Shear modulus modification factors of the near-field soil for the 30-story building and different earthquakes, for the soil type D.

Record no.	Modification factor	
	30-Story, Site I	30-Story, Site II
D1	0.74	0.69
D2	0.77	0.73
D3	0.75	0.72
D4	0.76	0.70
D5	0.74	0.68
D6	0.77	0.68
D7	0.76	0.69
D8	0.76	0.71
D9	0.76	0.71
D10	0.77	0.68

Fig. 12. The shear modulus modification factor versus the fixed-base fundamental period for each structure on each site averaged over the records. (a) Soil type C, (b) soil type: D, (c) soil type E.

9. Comparison of structural responses with different soil modeling procedures

In this section, the structural responses are calculated and compared for several cases of structures with different soil modelings discussed in this paper, including: elasto-plastic, traditional ELM, and the ELM modified for the near-field effects in this study.

9.1. The lateral displacements of stories

The maximum lateral displacements of all stories of the buildings in all 10 earthquakes corresponding to each soil type are calculated for both with and without SSI cases. For the SSI cases, three different assumptions for the soil behavior discussed in this paper as elasto-plastic, traditional ELM, and the modified ELM, are taken separately in the analysis. The results of response calculations are called Plastic, ELM, and NFM as short names for the above three modeling approaches. These are presented concurrently in the figures for comparison. The average of the maxi-

mum responses with SSI under different earthquakes is called Δ_{nSSI} for the story n. These are then normalized to the corresponding values for no SSI (Δ_n). The results are illustrated in Figs. 13–15 for the soil types C, D, and E, respectively. The maximum normalized responses do not variate much for the two soil profiles. The

Table 8
The shear modulus ratios for different buildings and soil types.

Building	Soil type C	Soil type D	Soil type E
5S	0.96	0.95	0.91
10S	0.92	0.91	0.85
15S	0.88	0.84	0.77
20S	0.86	0.82	0.74
25S	0.83	0.77	0.69
30S	0.80	0.73	0.64

maximum difference between the two sites for structural displacements proves to be only 9%. Because of the similarity of responses in the two sites and the large volume of results, the responses are presented as average of the two soil profiles. In the following figures, $\alpha_{\Delta n} = \Delta_{n SSI}/\Delta_n$.

The trend of displacements is predicted similarly by all three soil modeling assumptions. On the other hand, the amplitudes of NFM are less deviated from the plastic modeling than those of the ELM, especially for the buildings having up to 20 stories. The

Table 9
Coefficients of Eq. (2).

Soil type	A_1	A_2	B_1	B_2	C_1	C_2
C	− 0.0114	0.0047	0.0663	− 0.0330	− 0.1202	0.0312
D	− 0.0149	0.0067	0.0898	− 0.0569	− 0.1530	0.0355
E	− 0.0181	0.0077	0.1160	− 0.0573	− 0.2012	0.0608
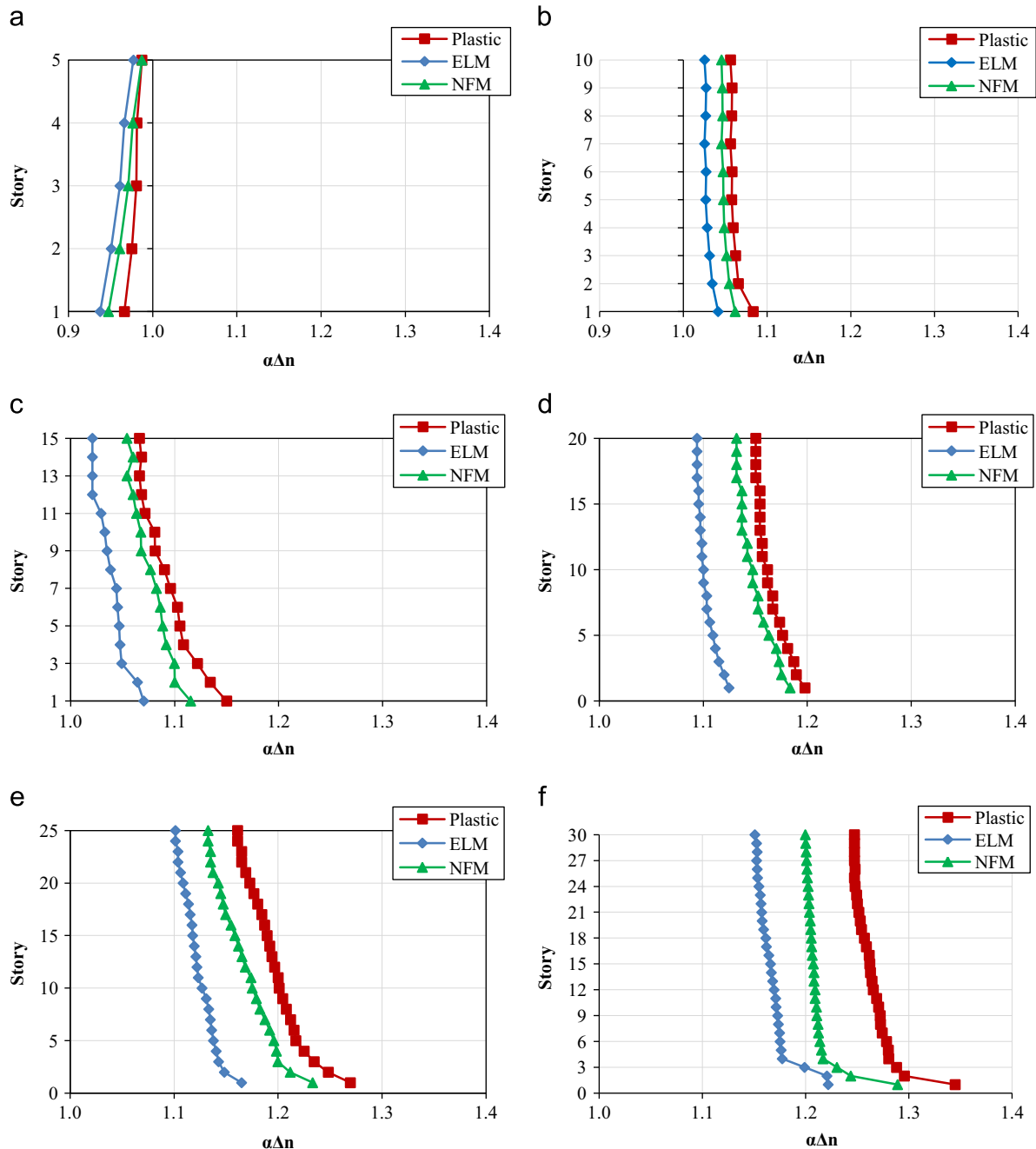
Fig. 13. Maximum lateral displacements of stories with SSI averaged between earthquakes and between the two soil profiles, normalized to those without SSI, soil type C. (a) 5-story building, (b) 10-story building, (c) 15-story building, (d) 20-story building, (e) 25-story building, (f) 30-story building.
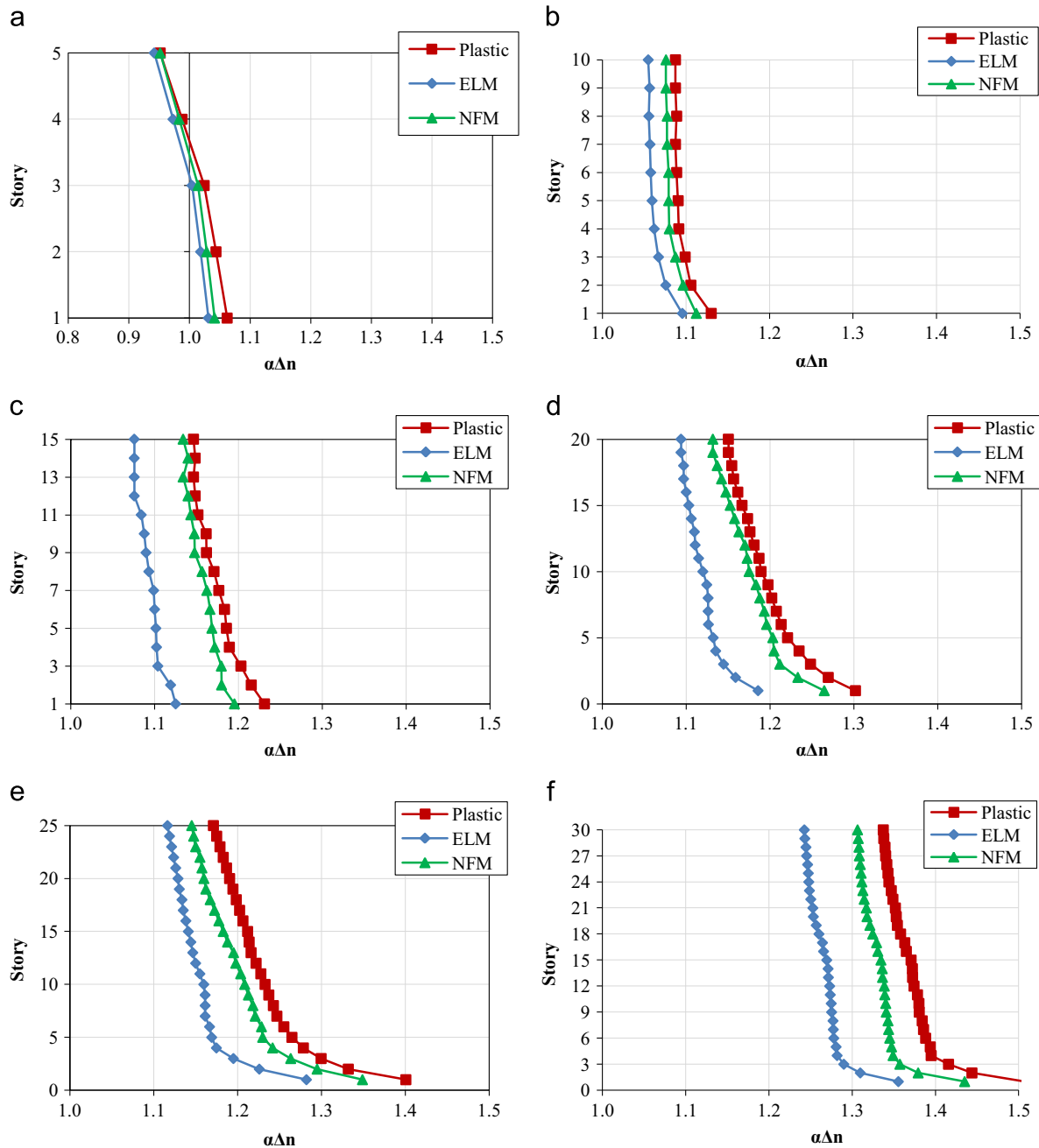
Fig. 14. Maximum lateral displacements of stories with SSI averaged between earthquakes and between the two soil profiles, normalized to those without SSI, soil type D. (a) 5-story building, (b) 10-story building, (c) 15-story building, (d) 20-story building, (e) 25-story building, (f) 30-story building.

maximum relative difference between the NFM (ELM) responses and those of the plastic model at identical levels of the 5, 10, 15, 20, 25 and 30-story buildings for the average of the two sites are respectively 2.0 (3.1), 2.1 (4.0), 3.0 (5.1), 3.0 (6.4), 3.3 (8.5), and 4.4% (10.2%) on the soil type C, 2.0 (4.9), 2.3 (7.0), 3.7 (9.1), 3.9 (10.4), 4.0 (11.5) and 5.1% (13.1%) on the soil type D, and 2.2 (6.1), 1.0 (8.0), 4.0 (9.1), 4.1 (11.4), 3.9 (13.5) and 5.3% (15.2%) on the soil type E.

In the above figures, in most cases, the plastic modeling of soil has resulted in increased lateral displacements of stories that is something intuitively predictable. Here it should be emphasized again that what is important here is the same phenomenon, i.e. SSI and increase of story displacements due to soil plasticity, not a strictly exact modeling of soil's nonlinear behavior that is impractical in the

presence of a large structure. It is observed that except of the 5-story building on the soil type C, the lateral displacement of stories is increased due to SSI relative to the no-SSI case. The increase is larger for lower stories, softer soils, and taller buildings and can reach values as much as 66%. At the upper stories the increase is smaller and even for the 5-story building the maximum displacements are less than those with SSI. At the same location, for the other cases the displacement increases between 0% and 40% with SSI. The variation is again larger for taller buildings on softer soils. For the 5-story building, rotation of foundation cannot increase the lateral displacement considerably and the response decreases or increases slightly based on the floor level and the soil type. This phenomenon shows how the rocking motion is important in increasing the lateral displacements of taller buildings.
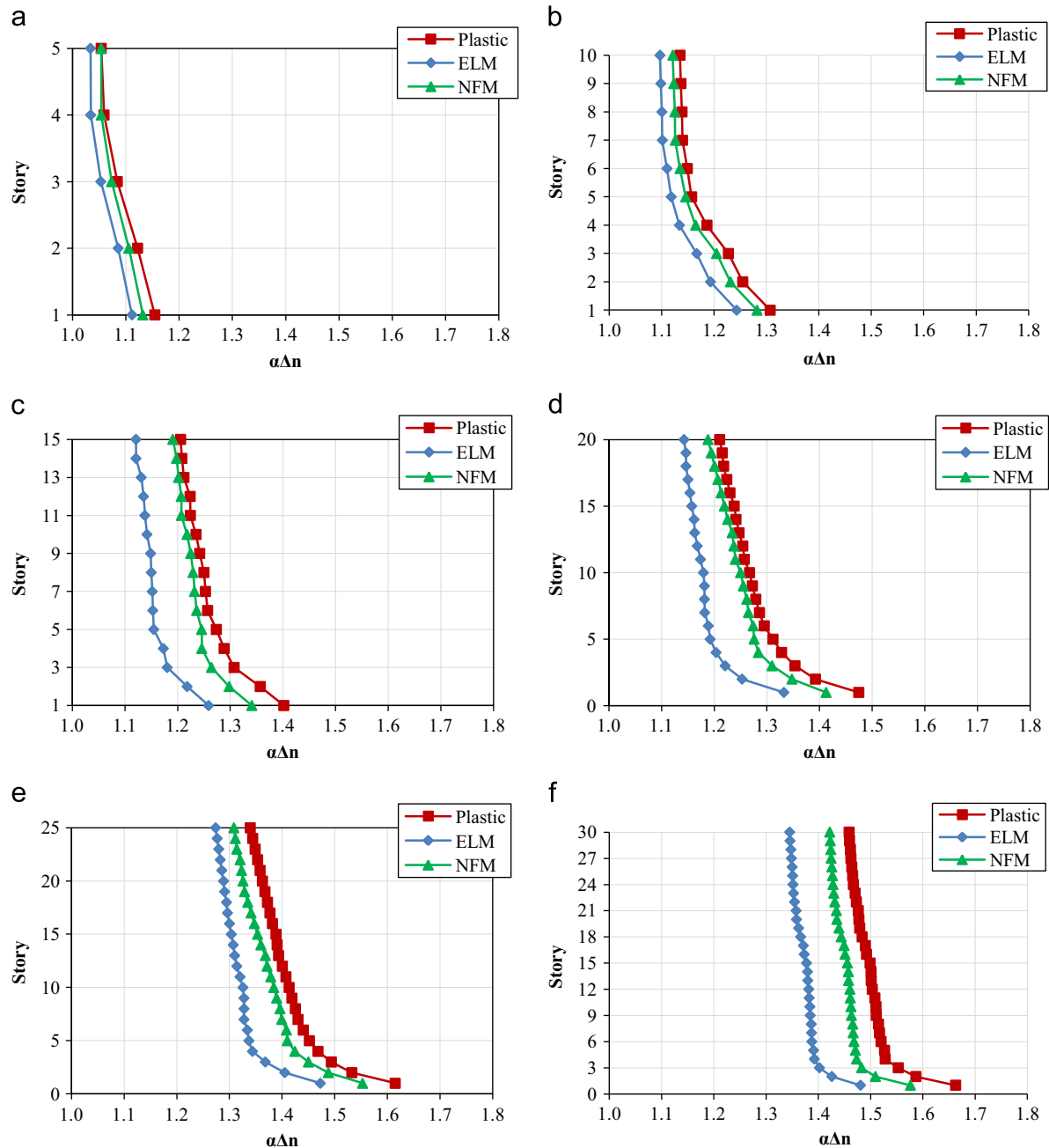
Fig. 15. Maximum lateral displacements of stories with SSI averaged between earthquakes and between the two soil profiles, normalized to those without SSI, soil type E. (a) 5-story building, (b) 10-story building, (c) 15-story building, (d) 20-story building, (e) 25-story building, (f) 30-story building.

9.2. The story shears

The story shears of each building are calculated for each earthquake and their maxima are averaged among the earthquakes for each soil type on each site. This calculation is carried out once with SSI on both sites, with three different soil modeling procedures as described above, and once without SSI. Finally, the story shears with SSI are normalized to their corresponding values without SSI and are called α_{Vn}. The results are shown in Figs. 16–18 for the soil types C, D, and E, respectively.

In Figs. 16–18, reduction of story shear due to SSI happens with no exception. This is in contrast to the displacement where it increased in most cases with SSI. The reduction in story shear is larger for upper stories, taller buildings and softer soils, and varies between 10% and

55% for the top story and 0% and 40% for the base shear. It is to be mentioned that the maximum allowable reduction in the design base shear with SSI is 30% according to ASCE7. It is interesting to note that plastic modeling of soil has resulted in the least story shears between the three soil modeling approaches unanimously. This is again intuitively expected because due to plasticity, a softer underlying soil results in a larger natural period and damping ratio and a smaller base shear for the building. The response amplitudes are similar for Plastic and NFM methods while ELM is more different compared with the NFM. This is while the NFM approach is a linear and much less time consuming than the plastic approach of the underlying soil modeling. The maximum relative difference between the NFM (ELM) responses and those of the plastic model at identical levels averaged between the earthquakes and the two sites for the 5, 10, 15, 20, 25 and 30-story
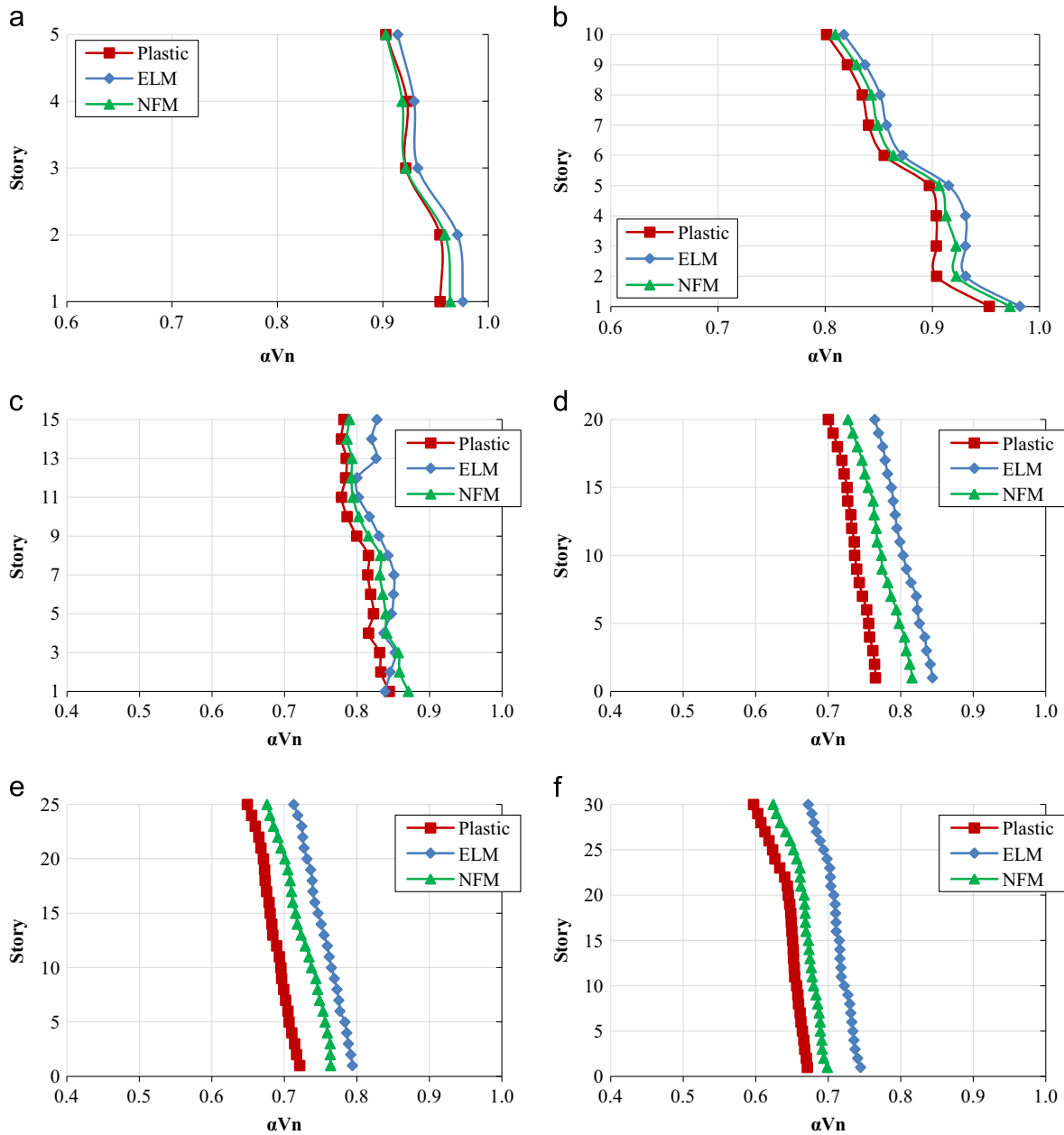
Fig. 16. Maximum story shears with SSI averaged between earthquakes and between the two soil profiles, normalized to those without SSI, soil type C. (a) 5-story building, (b) 10-story building, (c) 15-story building, (d) 20-story building, (e) 25-story building, (f) 30-story building.

buildings are respectively 1.6 (2.0), 2.1 (2.7), 3.2 (4.4), 3.6 (5.5), 3.1 (7.8), and 5.2% (8.1%) for the soil type C, 2.0 (3.0), 2.0 (4.5), 3.1 (6.1), 4.2 (8.2), 4.5 (9.5), and 5.4% (10.8%) for the soil type D, and 2.1 (5.1), 2.3 (7.3), 2.1 (9.1), 4.2 (11.2), 3.8 (12.4), and 5.8% (13.8%) for the soil type E.

10. Conclusions

The major goal of this research was developing a simple method for modeling the underlying soil with more accuracy in SSI analysis. For this purpose, a simple approach called the near field method (NFM) was developed in which an equation for further reduction of soil's shear modulus in a rectangular area below the foundation was presented through analysis of a nonlinear soil–structure system for earthquake records scaled to a

sample design spectrum. The accuracy of the proposed model was evaluated with several cases of structural response computations including lateral displacements and story shears of 5, 10, 15, 20, 25 30-story buildings on two soil profiles corresponding to the soil types C, D, and E. On each soil type, 10 consistent earthquake records were considered. While one of the two soil profiles was composed of sand and the other of clay, as the average shear wave velocity was almost the same in both sites, similar SSI trends were observed for the same building and soil type on both profiles. Therefore the soil profiles can be viewed upon as general enough within the soil types considered. The underlying soil was modeled in three different ways, including elasto-plastic Mohr–Coulomb modeling, traditional equivalent linear method (ELM), and the modified ELM (or the NFM approach) proposed in this study as described above. The structural responses were much more similar
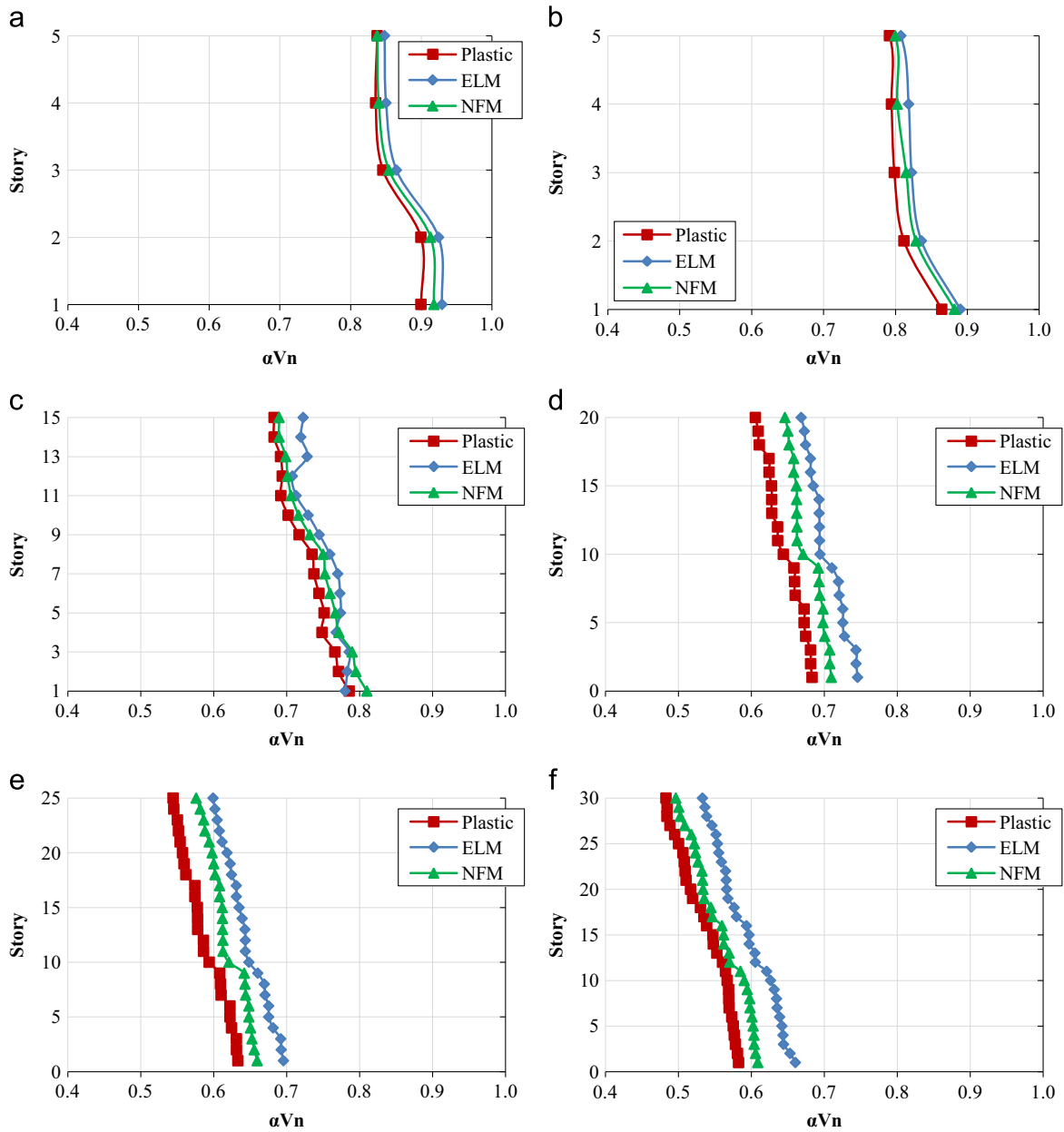
Fig. 17. Maximum story shears with SSI averaged between earthquakes and between the two soil profiles, normalized to those without SSI, soil type D. (a) 5-story building, (b) 10-story building, (c) 15-story building, (d) 20-story building, (e) 25-story building, (f) 30-story building.

to those of the plastic soil modeling with the NFM approach than the ELM, showing the suitability of the suggested method to predict maximum lateral displacements and story shears including SSI. The results were presented as graphs showing SSI responses normalized to those without SSI. These graphs can be used for converting the fixed-base design responses to those with SSI, at least for preliminary evaluation. Also, regression equations were derived for the reduced equivalent shear modulus with SSI, at the design spectrum level.

Moreover, in this study it was observed that

1) The reduced equivalent shear modulus of soil in the vicinity of foundation is smaller than the equivalent shear modulus of soil in the free-field analysis (of Shake). The ratio is from 96% to 64% for the soil types C, D, and E and the 5 to 30-story buildings, with its value being smaller for taller buildings on softer soils.

2) In the vicinity of surface foundations or pile caps, the maximum seismic strains of soil exceed the limit of validity of the equivalent linear method, and form a plastic zone.

3) Shape of the plastic zone of soil is more or less a function of the transverse dimension of foundation (or structure) and can be contained in a rectangle projecting 25% of the foundation width from both lateral sides and to the depth.

4) In all of the cases of soil modeling in this study, it is observed that distribution of SSI effects along structure's height is in the form of always decreasing story shears but increasing lateral displacements for taller buildings.
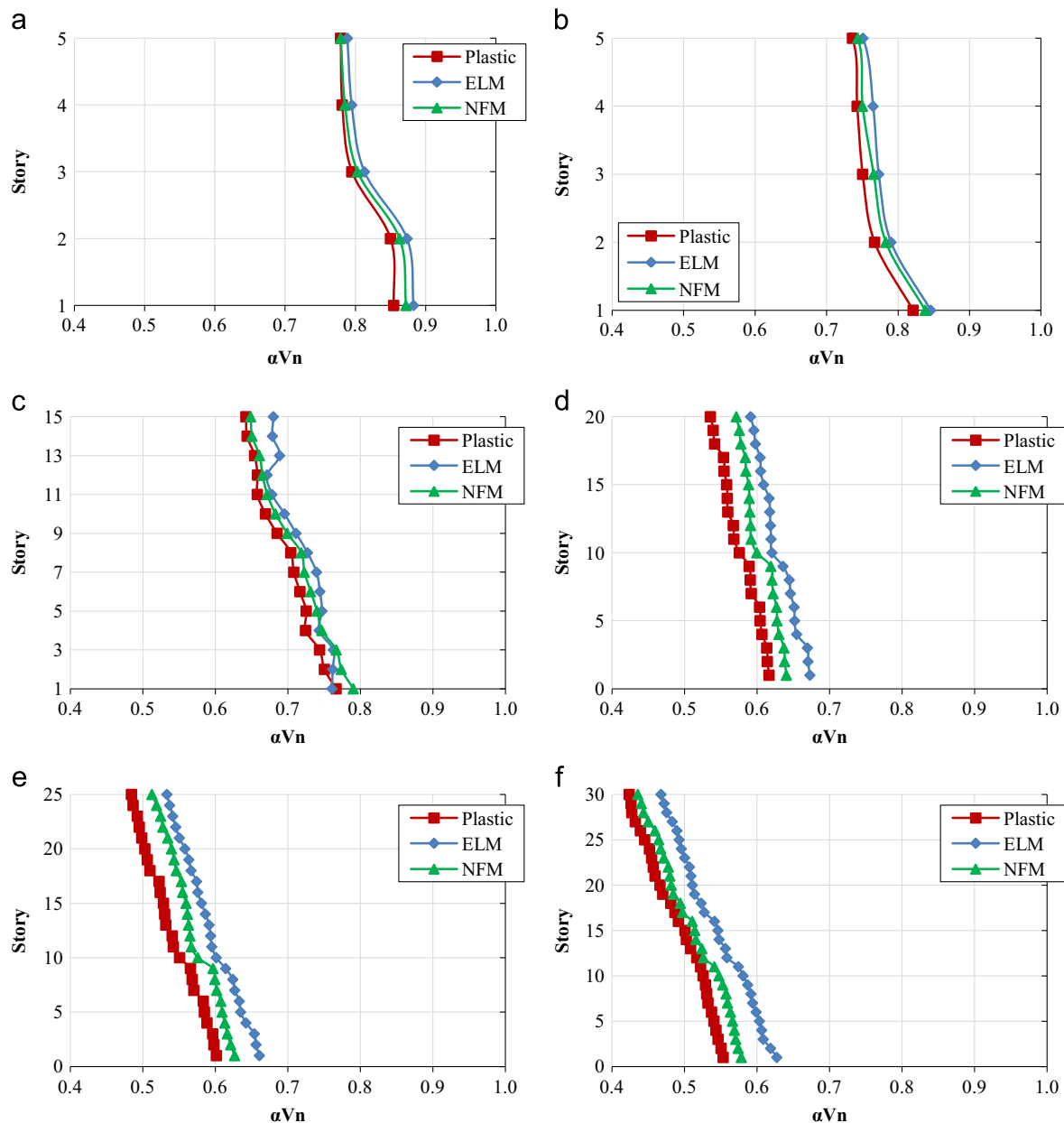
Fig. 18. Maximum story shears with SSI averaged between earthquakes and between the two soil profiles, normalized to those without SSI, soil type E. (a) 5-story building, (b) 10-story building, (c) 15-story building, (d) 20-story building, (e) 25-story building, (f) 30-story building.

References

[1] Wolf JP. The scaled boundary finite element method. Chichester: John Wiley & Sons Ltd; 2003.

[2] Casciati S, Borja RI. Dynamic FE analysis of South Memnon Colossus including 3D soil-foundation-structure interaction. Comput Struct 2004;82:1719–36.

[3] Emani PK, Maheshwari BK. Dynamic impedances of pile groups with embedded caps in homogeneous elastic soils using CIFECM. Soil Dyn Earthq Eng 2009;29:963–73.

[4] Manna B, Baidya DK. Dynamic nonlinear response of pile foundations under vertical vibration-theory versus experiment. Soil Dyn Earthq Eng 2010;30:456–69.

[5] Dutta SC, Bhattacharya K, Roy R. Response of low-rise buildings under seismic ground excitation incorporating soil-structure interaction. Soil Dyn Earthq Eng 2004;24:893–914.

[6] Wegner JL, Yao MM, Zhang X. Dynamic wave-soil–structure interaction analysis in the time domain. Soil Dyn Earthq Eng 2005;83:2206–14.

[7] Nakhaei M, Ghannad MA. The effect of soil–structure interaction on damage index of buildings. Eng Struct 2008;30:1491–9.

[8] Chau KT, Shen CY, Guo X. Nonlinear seismic soil–pile–structure interactions: shaking table tests and FEM analyses. Soil Dyn Earthq Eng 2009;29:300–10.

[9] Gajan S, Raychowdhury P, Hutchinson TC, Kutter BL, Stewart JP. Application and validation of practical tools for nonlinear soil-foundation interaction analysis. Earthq Spectra 2010;30:111–29.

[10] Pitilakis D, Clouteau D. Equivalent linear substructure approximation of soil–foundation–structure interaction: model presentation and validation. Bull Earthq Eng 2010;8:257–82.

[11] Raychowdhury P. Seismic response of low-rise steel moment-resisting frame (SMRF) buildings incorporating nonlinear soil–structure interaction (SSI). Eng Struct 2011;33:958–67.

[12] Romero A, Galvín P, Domínguez J. 3D non-linear time domain FEM–BEM approach to soil–structure interaction problems. Eng Anal Bound Elem 2013;37:501–12.

[13] ASCE7-2010. Minimum design loads for buildings and other structures. Virginia: ASCE; 2010.

[14] NIST GCR 12-917-21. Soil–structure interaction for building structures. Gaithersburg: National Institute of Standards and Technology, US Department of Commerce; 2012.

[15] Seed HB, Idriss IM. Soil module and damping factors for dynamic response analysis. Berkeley: University of California; 1979.

[16] PEER strong ground motion database. ver. 2010. ⟨http://peer.berkeley.edu/smcat/search.html⟩; [25.08.10].

[17] Computers & Structures, Inc.. SAP2000, linear and nonlinear static and dynamic analysis and design of three-dimensional structures. User manual. Version 11. Berkeley: University of California; 2006.

[18] Schnabel PB, Lysmer J, Seed HB. Shake-A computer program for response analysis of horizontally layered sites. report No. EERC 72-12. Berkeley: Univ. of California; 1972.

[19] Kramer SL. Geotechnical earthquake engineering. New Jersey: Prentice-Hall; 1996.

[20] Wolf JP. Dynamic soil–structure interaction. New Jersey: Prentice-Hall; 1985.

[21] Lin JW, Chen CW, Chung SH. Modeling and assessment of bridge structure for seismic hazard prevention. Nat Hazards 2012;61(3):1115–26.

[22] Cong Z, PWTZH Shiwei, Jianrong Y. Aseismic performance analysis of a certain sluice based on SAP2000. J China Three Gorges Univ (Nat Sci) 2009;5:006.

[23] Ghosh S, Wilson EL. Dynamic stress analysis of axi-symmetric structures under arbitrary loading. Berkeley: University of California, EERC; 1969.

[24] Ishihara K. Soil behavior in earthquake geotechnics. Oxford: Clarendon Press; 1996.

[25] PA. Vermeer. Plaxis: A finite element code for soil and rock analyses. Netherlands: AA Balkema Pub; 1998.

[26] Dassault Systems. Abaqus user manual. Version 6.8-1. Abaqus Inc.; Waltham, 2008.